Iranian Journal of Remote Sensing & GIS. *2026, 18 (2): 175-198* P-ISSN: 2008-5966, E-ISSN: 2588-6185

Original Article

Ecological Footprint and Biosustainability Assessment in Natural Mangrove Habitats of Iran

Parvaneh Sobhani*[1] and Afshin Danehkar[2]

Affiliation

1. *Dep of Environmental Science, Natural Resources Faculty, Lorestan University, Khorramabad, Iran.*
2. *Dep of Environmental Science, Natural Resources Faculty, University of Tehran, Karaj, Iran.*

ABSTRACT

Unfortunately, today, mangrove forests are facing many threats due to population growth and excessive development of human activities under the influence of local economic pressures, biophysical drivers, and socio-ecological systems, which have led to the vulnerability and destruction of these natural ecosystems. In the present study, to investigate possible future changes and uncertainties, land use/land cover (LULC) classes and their change trends were identified during the years 1989 to 2024. In addition, the change trend in 2050 was predicted and modeled using a Markov chain model and autonomous cells (CA-Markov). Next, the ecological footprint (EF), biocapacity (BC), and ecological deficit (ED) were calculated, and the level of function and equivalence factors (EQF) in this region was examined. Finally, the ecological pressure index (EPI) and ecological sustainability index (ESI) were also examined. According to the results, the area of Iran's mangrove forests in 2024 (131.25 km2 and 0.43%) decreased compared to 1989 (135.54 km2 and 0.44%). Among the existing LULC classes, built-up areas (with an area of 14032.32 km2 and 46.40%) have the highest increasing trend, while pastures (with an area of 11438.62 km2 and 37.82%) have the highest decreasing trend from 1989 to 2024. The results also indicate that built-up areas in 2050 have the largest increasing trend with an area of 11415.26 km2 among land classes. Overall, the EF in Iranian mangrove forests (during the years 1989–2024) has an increasing trend, and the BC and EP have also a decreasing trend. According to the results, the EDI also has an increasing trend, which indicates an increase in the intensity of natural resource consumption and a decrease in capital accumulation during the years under study. The results indicate an increase in EP and a decrease in sustainability in the area. Therefore, achieving sustainable development and protecting natural resources, as well as establishing a balance between human resource consumption and the absorption of waste produced by nature, requires the performance of planners and officials in preserving and supporting these natural habitats, in a way that they strive to preserve the resources with their biological value and improve the conservation status of these forests.

Keywords: Temporal-spatial changes, CA-Markov model, ecological footprint, biosustainability, mangrove forests of Iran.

* Corresponding Author: sobhani.pa@lu.ac.ir
DOI: https://doi.org/10.48308/gisj.2026.242171.1310
Received: 2025.10.24
Accepted: 2026.07.14

Copyright: © 2026 by the authors. Submitted for possible open access publication under the terms and conditions of the Creative Commons Attribution (CC BY) license https://creativecommons.org/licenses/by/4.0/).

1. Introduction

The increasing pressure of human activities, such as land use/land cover (LULC) changes and unplanned productivity to achieve economic and commercial benefits, requires integrated planning and management at all levels to protect land and its valuable biological resources (Sobhani et al., 2021; Wassie, 2020). Furthermore, in the establishment of uses and development of activities, the need for optimal exploitation of land resources along with basic protection and prevention of their destruction, to achieve sustainable development, is essential (Sobhani & Esmaeilzadeh, 2021). LULC changes, which include direct and indirect human interventions, can seriously change approximately half of the land surface of the Earth (Xie et al., 2024; Oli et al., 2025). Therefore, LULC is one of the most important factors that humans can affect their environment, and knowing how these changes play a significant role in land management and planning (Nuissl & Siedentop, 2021; Gabisa et al., 2025).

Understanding the ecological conditions governing natural ecosystems is essential for achieving sustainable development (Zadehdabagh et al., 2022). The Ecological Footprint Index (EFI) is widely used to measure sustainability levels in these areas (Shamaee et al., 2024; Genta et al., 2022). By providing a comprehensive comparison of the demand and supply of natural resources, this index examines useful goals and strategies for preventing the destruction and inequalities of human activities (Yadav et al., 2023). In this regard, forest ecosystems, if properly managed, can provide functions such as maintaining ecological and life-giving processes, genetic diversity, and providing habitat for sensitive species and many other services (Wang et al., 2025).

Unfortunately, today, mangrove forests are facing numerous threats due to population growth and the excessive development of human activities under the influence of local economic pressures, biophysical drivers, and socio-ecological systems, which have led to the vulnerability and destruction of these natural ecosystems. Research indicates that from 1996 to 2020, more than 24.5 km2 (3.4%) of mangrove cover was lost due to urbanization, agriculture, and aquaculture development in coastal environments, and the ecological sustainability trend in these valuable biological habitats has been affected by human activities (Rondon et al., 2023). Despite the high importance of mangrove forests in providing ecosystem services and human needs, the destruction and loss of these unique coastal habitats have intensified worldwide, as a large part of these forests has been degraded and degraded, and this trend continues (Tran et al., 2024). Accordingly, examining the EFI in these natural habitats is one of the most important tools available for assessing biological sustainability and providing effective management solutions to reduce adverse effects and achieve the goal of protecting mangrove forests (Galdavi et al., 2025).

The ecological footprint approach aims to establish a balance between "resource consumption and waste production by humans" and "resource production and waste absorption by nature" (Skakovska, 2023). Today, the EFI is used in many countries around the world at national and local levels, indicating where and in which areas natural resources are under pressure (Li et al., 2023). The ecological footprint, emphasizing the limitations of capital and land resources, has become popular as a framework for impact assessment and sustainable planning and has attracted the attention of many researchers (Sarwar et al., 2024).

To achieve sustainable development in natural ecosystems, this index has been used in numerous studies and research (Yang et al., 2024; Muhirwa et al., 2025; Khezri et al., 2023). Given the importance of this issue, the present study examined some of these studies, including the study by Sobhani and Danehkar (2024) on assessing changes in natural capital and the level of ecological sustainability in the mangrove protected area. According to the results, the ecological footprint shows an increasing trend, while the biological capacity shows a decreasing trend. Thus, the EFI has increased during 1989-2021, indicating high intensity of use of mangrove resources and forests. In another study, Arifanti et al. (2025) assessed the environmental and socio-economic impacts of Indonesian mangrove forest loss and the ecological footprint of mangroves. Their results showed that the degradation and reduction of mangrove forests in this region is driven by the increasing demand for commodities, including shrimp, fish, rice, and other products. These activities ultimately lead to negative environmental impacts on mangrove forests and adjacent ecosystems and the livelihoods of coastal communities. To prevent further degradation, there is a need for a comprehensive system of mangrove forest conservation and restoration in Indonesia that can improve the livelihoods of local communities. Zheng et al. (2023) examined the conservation of mangrove forests in China based on the ecological footprint. The results showed that the average carbon footprint of mangrove forests is about 1000 million hectares, which is lower than other forest covers, while the biological capacity of these forests is not as high as expected due to the limited area of mangroves. Chamberland-Fontaine et al. (2022) also addressed the improvement of sustainable management of mangrove forests in Panama. The findings showed that socio-economic management at the local level requires a greater focus on ecological models and strategies to increase connectivity, cooperation, and a more coherent perspective for the utilization of coastlines. Moreover, the depth of the ecological footprint of the economic belt of this region is possible through balancing the industrial structure and improving sustainable development.

According to studies conducted, sustainable development emphasizes the sustainability of natural resources and valuable biological reserves, which can be achieved by measuring the ecological footprint and creating a balance between human resource consumption and the absorption of waste produced by nature. Therefore, in the present study, we calculated the ecological footprint (EF), biological capacity (BC), and ecological deficits (ED), and examined the level of function and ecological balance in Iranian mangrove forests.

Despite the importance of these natural habitats in providing valuable economic, social, and biological services and meeting the livelihood needs of local communities, they are being severely degraded and destroyed to make way for various aquaculture activities, industrial development, and urbanization. In this regard, considering the habitat values, forestry attractions, biodiversity richness, and especially the high tourism potential of the country's mangrove forests, they have attracted more attention from researchers, planners, and decision makers in the last two decades. Accordingly, in the present study, to examine possible future changes and uncertainties, the LULC classes and their change trends during the years 1989 to 2024 were first identified. In addition, the change trend in 2050 was predicted and modeled using a Markov chain model and autonomous cells (CA-Markov). Next, the EF, BC, ED, and the level of function and Equivalence Factors (EQF) and balance in this area were calculated. Finally, Ecological Pressure Index (EPI) and Ecological Sustainability (ESI) were also examined. The results of this study can help decision makers in long-term planning and also predict the trend of changes in the future.

2. Materials and Methods

2.1. Study Area

The Iranian mangrove forests are located in eight basins: Dayer-Bordkhon (Dayer and Bordkhon), Nayband Bay (Bidkhon and Basatin), Khamir (Sayeh Khosh, Khamir-Lashteghan, Mardo, and Pohl), Qeshm (Khorkhoran and Qeshm coast), Kolaghan-Kolahi (Kolaghan, Tiab, and Kolahi), Sirik (Sirik), Jask (Jask city, Shahr-Now, and Khalasi, and Gabrik), and Gwadar Bay (Khor baho and Khor Gwadar), in three provinces of Sistan and Baluchestan, Hormozgan, and Bushehr. The study area receives an average annual rainfall of 146 mm and has a mean annual temperature of 27.2°C. These natural habitats are recognized as major coastal nature-based tourism destinations and constitute one of the country's most important biodiversity hotspots, providing a wide range of ecosystem services (Sobhani & Danehkar, 2025). Fig. 1 illustrates the geographical location of the study area.

3. Methodology

3.1. Identifying and investigating the trend of LULC changes

In this study, multispectral images of the Landsat collection from different time periods (1989, 1999, 2009, and 2024) were used to show the spatial-temporal series of

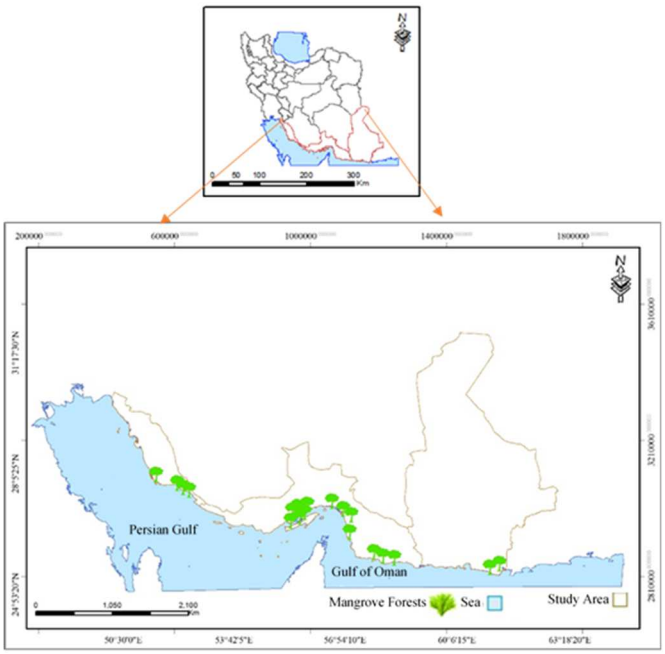


Fig. 1. Geographical location of the study area

LULC changes as well as the map of LULC classes in this region. The images studied included L5-TM for 1989 and 1999, L7-ETM+ for 2009, and L8 and OLI-TIRS for 2024. It should be noted that the reason for examining the aforementioned time periods is due to the five-year development after the revolution (types of physical-economic development), population growth, increased tourism demand, the expansion of human activities during this period, and the start of environmental studies in the country. Therefore, images from 1989 to 2024 were selected and examined. Furthermore, the month of preparing the images was May due to the dominant green cover and the flowering time of mangrove habitats in this time period. The Random Forest (RF) algorithm was used to classify the images. This algorithm, which is often used to classify satellite images in terms of spatial resolution, has achieved remarkable results compared to conventional classification algorithms based on support vector machines and neural networks and introduces new methods of hybrid classification (Ao et al., 2018; Zang et al., 2019). The RF method is a supervised classification method in which a set of trees is used in decision-making and classification. In this method, many decision trees that are most distinct from each other are first formed, and the decision-making process is examined separately for each of these trees. The RF is one of the machine learning methods that has attracted the attention of many researchers owing to its high speed on large volumes of data and the lack of need for training data (Fischer et al., 2023). In this method, the network parameters, including the number of trees and

nodes for each tree, are first determined. Then, a number of input data are randomly selected for each tree. After the decision-making operation in each of these trees, the results are combined (the classification output is generated based on a majority vote from the predictions of the single trained trees). The accuracy of this method is determined according to the power of the trees, individually, and the degree of correlation between them, meaning that the better the decision-making ability of the selected trees and the lower their degree of correlation, the higher the final accuracy will be. Next, change monitoring and image accuracy assessment were addressed. Highlighting and change monitoring are, in fact, the discovery of changes in a location, which is carried out in the remote sensing process using images from two or more times (Liu et al., 2007; Munthali et al., 2020). In the present study, the classification accuracy was also examined based on the kappa index and overall accuracy.

The Google Earth Engine (GEE) web-based system was used to process data and information. Thus, the maps of mangrove forest LULC classes during the years under study were extracted based on the Normalized Difference Index (NDWI) of water areas and classified into two classes: water and non-water. In this index, the visible green band and the near-infrared band were used to highlight water areas and remove vegetation and soil covers. The range of changes in this index is between +1 and -1, where the closer the pixel value is to +1, the presence of water areas is indicated, and the closer it is to -1, the presence of non-water areas is indicated (Sagar et al., 2017). Eq. 1 can be used to calculate this index. Given that in the present study, the images used included a set of LANDSAT satellite images, the visible green band was considered equivalent to band 3, and the near-infrared band was considered equivalent to band 5. In the prepared maps, the blue zone class was displayed with code zero and the non-blue classes with code one.

$$NDWI = \frac{(B3-B5)}{(B3+B5)} \quad (1)$$

NDVI was also used to extract mangrove cover from other LULC classes, according to Eq. 2. This index is one of the most widely used indices in remote sensing data, where R and NIR are the visible red and near-infrared wavelengths, respectively (Shimu et al., 2019). NDVI is a normalized value between -1 and +1, and areas with dense vegetation cover have high NDVI values because of relatively high reflectance in the near-infrared range and low reflectance in the visible red range.

$$NDVI = \frac{(NIR-R)}{(NIR+R)} \quad (2)$$

Because the study area is coastal and marine and has tidal and muddy areas, the normalized turbidity difference index (NTDI) was used to separate and differentiate the areas more accurately. Given that clear and

transparent waters within the green bands and especially the red band have very weak reflectance (less than 10%), these bands can be used to estimate and investigate muddy and tidal areas that lack transparency (Lacaux et al., 2007). This index was obtained using Eq. 3.

$$NDTI = \frac{(R-G)}{(R+G)} \quad (3)$$

Next, the Soil Adjusted Vegetation Index (SAVI) was used to adjust the soil effect and distinguish mangrove forest covers. This index uses the red and infrared bands to extract vegetation cover. The SAVI uses a coefficient called the soil effect modifier, which reduces the soil effect. According to Eq. 4, the coefficient L has an inverse relationship with the vegetation density and is between zero and one. In this relationship, the greater the vegetation cover, the closer L will be to zero, and vice versa (Xia et al., 2020).

$$SAVI = (1 + L) * \left[\frac{(NIR-R)}{(NIR+R+L)}\right] \quad (4)$$

3.2. Selection of training samples

Sampling is one of the most important steps in image classification and has a significant impact on the quality and accuracy of the classification. In this study, sampling points in the GEE web-based system were selected visually in a desired number and randomly selected. A maximum of 1500 samples were selected, of which 800 were used to train the algorithm and 700 were used to test the classification (the number of samples for each LULC class included croplands and gardens (150 samples), water areas (150 samples), pastures (300 samples), forests (man-planted) (150 samples), mangrove forests (300 samples), built-up areas (300 samples), and bare land (150 samples)). It is worth noting that to prevent overfitting due to spatial autocorrelation, training and evaluation samples were selected independently, and test samples were not extracted from the same polygons or training pixels. The satellite images were then classified, and LULC maps were prepared using the RF algorithm (10 decision trees were examined according to the training data), as described above. Based on this, a map of LULC classes in the study area was identified and prepared in seven classes: croplands and gardens, water areas, pastures, forests (man-planted), mangrove forests, built-up areas, and bare lands.

3.3. Forecasting and modeling the trend of LULC changes in 2050

3.3.1. Markov chain model and autonomous cells (CA-Markov)

Today, changes and transformations of LULC are known as a threat factor in mangrove forests (Sobhani & Danehkar, 2024). Therefore, monitoring these changes through satellite images and predicting and assessing their potential through modeling can help environmental planners and natural resource managers make more informed decisions and foresight in planning (Sobhani et al., 2021). Accordingly, in the present study, after examining and mapping LULC

changes, to plan and make decisions in the long term and also predict the trend of changes in the future, modeling and predicting LULC changes in 2050 was attempted using the CA-Markov model and Idrisi TerrSet 2020 software with a cell size of 30*30. CA-Markov serves as a tool to describe changes and processes in ecosystems in the future. This model also interprets LULC changes from one period to another and uses them as a basis for mapping future changes, which is done using a transition probability matrix from time 1 to time 2 (Arkhi & Esfahani, 2019). Markov chain analysis was performed in this study for two purposes: 1) to prepare the first matrix (transition probability matrix) for model calibration by simulating the land cover-use map of 2024 using the 1989 map, and 2) to prepare the second matrix to predict the land cover-use change map in 2050 using the simulated map in 2024. In addition, to measure the accuracy of the modeling, the simulated map of 2024 was compared with the actual map. Since the most common parameters for estimating accuracy are overall accuracy and kappa coefficient (Lu et al., 2004), in this study, the measurement of the accuracy of the information was examined through the kappa coefficient, and finally, the simulated land cover-use map using the CA-Markov model in 2050 was obtained according to the accuracy of the examined information. In accordance with the Bayesian probability formula, Eq. 5 was used to predict land use changes in the Markov chain model (Sang et al., 2011).

$$S_{(t+1)} = P_{ij} * S_{(t)} \quad (5)$$

In this relation, S(t) and S(t+1) are the states of the system at times t and t+1, respectively, and Pij is the transition probability matrix in these states, which is calculated using Eq. 6.

$$\begin{pmatrix} P_{11} & \dots & P_{1n} \\ \vdots & \ddots & \vdots \\ P_{n1} & \cdots & P_{nn} \end{pmatrix} P_{ij} \geq 0, \sum_{j=1}^{n} P_{ij} = 1, j = 1, \dots, \dots, n \quad (6)$$

Next, an autonomous cell model was used, in which the space was defined as a grid, with each cell called a cell. Autonomous cells are synchronized at discrete times and according to a local rule, where the value of each cell is determined based on the values of the neighboring cells and the cell itself (Aslami et al, 2015). Therefore, the autonomous cell model can be calculated from Eq. 7 (Sang et al., 2011). In this Eq, S is a set of cell states, N is the cell context, t and t+1 represent state changes at different times, and f represents a transfer function in cell states and local space.

$$S(t, t+1) = f(S(t), N) \quad (7)$$

In the present study, variables such as altitude, slope, direction, population density, distance from roads (access roads), and distance from residential areas were examined as driving factors of change based on regional conditions and expert opinions using the Idrisi TerrSet software.

3.3.2. EF Assessment

After identifying the LULC classes using satellite images in the region, the ecological footprint was calculated according to Table 1 and based on a global system in gha. Accordingly, each class was converted to global hectares (gha) based on Equivalence Factors (EQF) and Yield Factors (YF), and then EF and BC were calculated based on these values. In the present study, each of the land cover/use classes in Iranian mangrove forests was considered as the main resource for measuring the ecological footprint. In this classification, biological resources were divided into three categories: agricultural products (irrigated agriculture and rainfed agriculture), pasture products (dense pastures, semi-dense pastures, and low-density pastures), and forest products (man-planted forests, low-density forests and shrublands, and sparse forests). Energy in this region includes carbon capture and fossil fuels, and pollutants are allocated to greenhouse gas emissions. In addition, the built-up areas in this region include man-made areas such as rural population centers, residential towns, city limits, facilities, and cemeteries.

EF calculations depend on the level of local economic production, total population, and degree of regional development. It is performed for various consumption resources in relation to the area of the relevant biological productive land. In contrast, the EF model balances and simplifies the supply and demand of biological production space within complex ecological and economic processes (Li et al., 2023). Its measurement unit is based on the global average unit in ha (gha), as it specifically refers to the performance of biological products on a global scale. The gha indicates the ha in the potential of biomass production equivalent to the global average in that year (Fang et al., 2014). For this purpose, the global average production can be calculated using Eq. 8, where Epj: global average product; pj: global

Table 1. Data sources and details (https://data.footprintnetwork.org)

Factors	Indicators
Biological account	Agricultural products (such as cereal, beans, tubers, cotton, oil-bearing crops, fiber crops, tobacco, sugarcane, etc.) Grass products (such as beef, lamb, milk, wool, cashmere and honey) Forest products (such as wood, tea and garden fruits) Aquatic products (such as shrimps, crabs and fish)
Water account	Total water consumption in agriculture, industry, living and ecology activities
Energy account	Consumption of various energy and fossil fuels, including coal, coke, petroleum, crude oil, gasoline, kerosene, diesel oil, fuel oil, liquefied petroleum gas, natural gas and electricity
Pollution account	Release of pollutants including COD, NH3-N, SO2, NOx and solid waste
Built-up areas	The price of major farm products

product; and sj: the global production level of biological resource generator in class j.

$$E_{pj} = \frac{p_j}{s_j} \quad (8)$$

In calculating the EF, any ecosystem service, regardless of whether it is locally produced, imported, or exported, can be allocated to the area of bioprotective land using Eq. 9 (Yang, 2018; Mancini, 2018; Galli, 2020). Where EFc is the total EF of consumption, ef is the per capita ecological footprint, N is the total population, i is the product category, Ci is the per capita consumption of product i, Ywi is the average global yield of product i, and EQFi is the LULC class equivalence factor for product i.

$$EF_c = N \times ef = N \times \sum_i^n (\frac{C_i}{Y_{w,i}} \times EQF_i) \quad (9)$$

- Carbon footprint (CF): This represents the output of the EF model, which calculates the demand for long-term sequestration of CO2 emissions by forest ecosystems. The CF is calculated using Eq. 10. In the following Eq., EFc is the EF component, i.e., the land area required to absorb CO2 from fossil fuel combustion, Pc is the annual CO2 emission rate, and Yc is the annual carbon sequestration rate per global average ha of forest land, equivalent to 3.67 tons per ha (Lin et al., 2018).

$$EF_c = \frac{2}{3} \times \frac{P_c}{Y_c} \times EQF \quad (10)$$

- BC: In this study, BC is divided into different land use types (LULC classes) that can produce essential renewable resources or absorb waste CO2 (ecosystem regulation services) and is calculated (Eq. 11). In this regard, BC represents the maximum flow of ecosystem services in the area. Thus, human demands for renewable resources and CO2 sequestration are met by the primary products or services of the LULC classes (Lazarus, 2015; Lin, 2015; Mancini, 2018). In addition, according to the World Commission on Environment and Development (WCED, 1987), 12% of bioprotective areas should be saved to maintain biodiversity and ecosystem integrity.

$$\mathrm{BC} = 0.88 \sum_i \mathrm{A_{N,i}} \times \mathrm{YF_{N,i}} \times \mathrm{EQF_i} \quad (11)$$

ANi is the biological production area available for the production of each product i, YFNi is the yield factor, and EQFi is the equivalence factor for the LULC producing each product i (Galli, 2020; Mancini, 2018). To examine the consumption of capital accumulation by flow (Rstok flow) and the occupation of capital flow (orflow), two indices, EFdepth and EFsize, are calculated according to Eq. 12 and 13 (Long, 2020; Bi, 2021; Wu, 2021).

$$\begin{aligned} \mathrm{EF_{depth}} &= 1 + \frac{\sum_i \mathrm{ED_i}}{\mathrm{BC}} = 1 + \frac{\sum_i \max(\mathrm{EF_i} - \mathrm{BC_i}, 0)}{\mathrm{BC}} \\ \mathrm{EF_{size,3D}} &= \min\{\mathrm{EF}, \mathrm{BC}\} \\ \mathrm{EF_{3D}} &= \mathrm{EF_{size}} \times \mathrm{EF_{depth}} \end{aligned} \quad (12)$$

To calculate EFsize for forests, Eq. 13 can also be used. In this Eq., EFdepth is the depth of the EF, EFsize is the size of the EF, ED is the ecological fraction, and the number 1 represents the natural depth.

$$EF_{sizeforestland} = \min\{EF_{forestland} + EF_{carbon}, BC_{forestland}\}$$
$$EF_{depthforestland} = 1 + \frac{\max\{EF_{forestland} + EF_{carbon}, BC_{forestland}, 0\}}{BC_{forestland}} \quad (13)$$

In this study, Rstok flow, orflow, and excess natural capital flow (EFremain) were examined and analyzed using EPI and ESI. EPI indicates regional consumption pressure and the status of ecosystem services in the region, and the larger this value is, the greater the EP (Yang & Hu, 2018). This index can be calculated using Eq. 14. Table 2 shows the classification of ecosystem status based on EPI.

$$EFI = \frac{ef}{bc} \quad (14)$$

ESI also indicates the extent to which a region's sustainable ecological supply can meet the ecological demand of the community. This index can be calculated using Eq. 15 (Muhirwa et al., 2025). The ESI value is in the numerical range [0 and 1], where the closer it is to 1, the more sustainable it is, and the closer it is to zero, the less sustainable it is, and ESI=0.5 represents the threshold between sustainable and unsustainable development.

$$ESI = \frac{ec}{ec+ef} \quad (15)$$

In addition, the Rstok flow is used to better understand the contribution of flow and accumulation in the use of natural capital; the higher the value of this index, the less sustainable the use of natural capital (Zhang, 2020). This index can be calculated using the following equation: 16.

$$R_{stockflow} = \frac{EF - EF_{sizeregion}}{EF_{sizeregion}} = \frac{ED}{BC} = EF_{sizeregion} - 1 (EF > BC) \quad (16)$$

In the present study, orflow was also used to describe the actual efficiency of human use of flow and analyze the overuse situation, which can be calculated using Eq. 17 (Bi, 2021). The EFremain for different land uses was also calculated according to Eq. 18 (Dong, 2021).

$$or_{flow} = \frac{EF_{size,i}}{BC_i} \times 100 \quad (17)$$

$$EF_{remain,i} = 1 - \{\min[EF_i, BC_i] BC_i\} \quad (18)$$

4. Results

4.1. Analysis of LULC changes

The results of the image accuracy assessment, as shown in Table 3, indicate that the obtained values are of high desirability and are at an acceptable level. As the results showed (Table 4), the area of Iran's mangrove

Table 2. Ecosystem status classification based on EPI (Liu et al., 2021a)

Level	1	2	3	4	5	6
EPI	<0.5	0.5-0.8	0.8-1	1.1-1.50	1.51-2	>2
Ecosystem service status	Completely safe	Very safe	Relatively safe	Relatively unsafe	Very unsafe	Completely unsafe

forests in 2024 (with an area of 131.25 km^2 and 0.43%) has decreased compared to 1989 (with an area of 135.54 km^2 and 0.44%). Among the existing LULC classes, built-up areas (with an area of 14032.32 km^2 and 46.40%) have the highest increasing trend, while pastures (with an area of 11438.62 km^2 and 37.82%) have the highest decreasing trend during the years 1989 to 2024. Water areas also show a decreasing trend during these years (with an area of 283.26 km^2 and 0.93%). Forests (man-planted) as another LULC class in this region have also shown an increasing trend (with an area of 1310.31 km^2 and 33.4%). Moreover, bare lands (with an area of 112.85 km^2 and 0.37%) have shown an increasing trend during the studied years (Table 4). Fig. 2 shows the trend of changes in LULC classes in the study area.

4.2. Prediction of LULC changes in 2050

According to the results, the obtained kappa coefficient is equal to 0.81, which confirms the accuracy of the model used in this study. As the results show, in the Iranian mangrove forests, the most decreasing trend in 2050 is related to pastures with an area of 11415.26 km2 (37.74%), while the largest increasing trend is related to built-up areas with an area of 14056.47 km2 (46.48%) (Table 5 and Fig. 3). This trend indicates the speed of development of human activities in these habitats and the conversion of LULC classes to built-up areas. Table 6 shows the transition probability matrix of the predicted LULC classes for 2050 based on the 2024 classification.

Table 3. Image accuracy assessment based on overall accuracy and kappa coefficient from 1989-2024

Satellite images	Year	Overall accuracy	Kappa coefficient
L5-TM	1989	0.93	0.85
	1999	0.95	0.88
L7-ETM+	2009	0.90	0.86
8, OLI-TIRS	2024	0.98	0.90

Table 4. LULC changes in the studied area from 1989-2024

Year	1989		1999		2009		2024		1989-
LULC classes	Area								
	Km^2	%	Km^2	%	Km^2	%	Km^2	%	Km^2
Croplands and gardens	2815.84	9.30	2845.31	9.40	2912.81	9.62	2932.96	9.69	117.12
Water areas	302.67	1.0	301.45	0.99	295.11	0.97	283.26	0.93	-19.41
Pastures	11808.74	39.04	11743.34	38.82	11618.23	38.40	11438.62	37.82	-370.12
Forests (man-planted)	1219.6	4.03	1223.11	4.04	1264.41	4.18	1310.31	4.33	90.71
Mangrove forests	135.54	0.44	134.88	0.44	134.75	0.44	131.25	0.43	-4.29
Built-up areas	13854.33	45.80	13886.62	45.91	13911.52	45.99	14032.32	46.40	177.92
Bare lands	109.87	0.36	110.54	0.36	111.87	0.36	112.85	0.37	2.98
Total	**30241.57**	**100**	**30241.57**	**100**	**30241.57**	**100**	**30241.57**	**100**	**-**

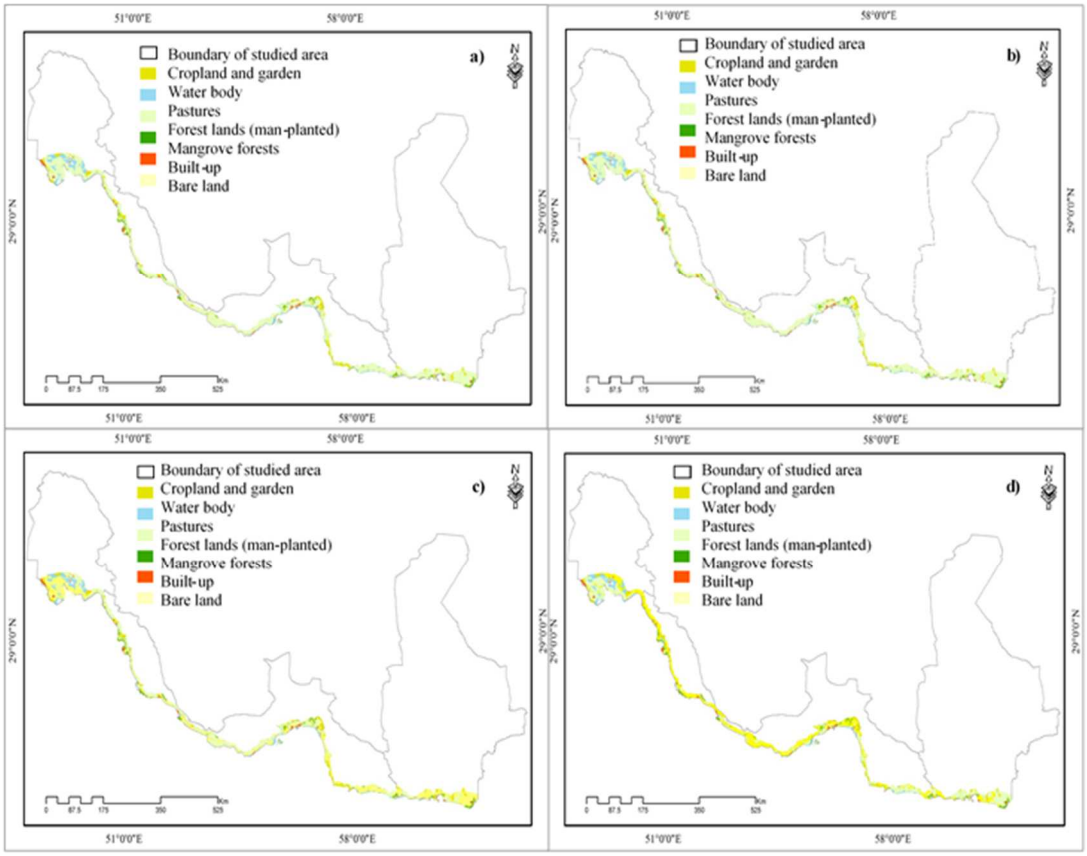


Fig. 2. LULC class map of Iran's mangrove forests in the years: a) 1989, b) 1999, c) 2009, d) 2024

Table 5. Forecast of LULC change trends using the CA-Markov model from 2024 to 2050

Year / LULC classes	Actual LULC area 2024		Simulated LULC area 2024		Simulated LULC area 2050		Decreasing/increasing trend
	Km²	%	Km²	%	Km²	%	
Croplands and gardens	2932.96	9.69	2931.86	9.69	2933.11	9.69	Increase
Water areas	283.26	0.93	280.87	0.92	280.27	0.92	Decrease
Pastures	11438.62	37.82	11436.72	37.81	11415.26	37.74	Decrease
Forests (man-planted)	1310.31	4.33	1316.21	4.35	1314.36	4.34	Increase
Mangrove forests	131.25	0.43	132.44	0.43	128.82	0.42	Decrease
Built-up areas	14032.32	64.40	14029.86	46.39	14056.47	46.48	Increase
Bare lands	112.85	0.37	113.61	0.37	113.28	0.37	Increase
Total	**30241.57**	**100**	**30241.57**	**100**	**30241.57**	**100**	-

Table 6. LULC class transition probability matrix for 2050 based on 2024 classification (%)

LULC classes	Croplands and gardens	Water areas	Pastures	Forests (man-planted)	Mangrove forests	Built-up areas	Bare lands
Croplands and gardens	0.956	0.001	0.012	0.003	0.000	0.024	0.004
Water areas	0.006	0.982	0.000	0.000	0.005	0.002	0.005
Pastures	0.021	0.000	0.947	0.006	0.000	0.018	0.008
Forests (man-planted)	0.004	0.000	0.018	0.962	0.000	0.11	0.005
Mangrove forests	0.000	0.007	0.002	0.001	0.985	0.003	0.002
Built-up areas	0.002	0.000	0.001	0.000	0.000	0.995	0.002
Bare lands	0.014	0.000	0.026	0.002	0.000	0.018	0.940

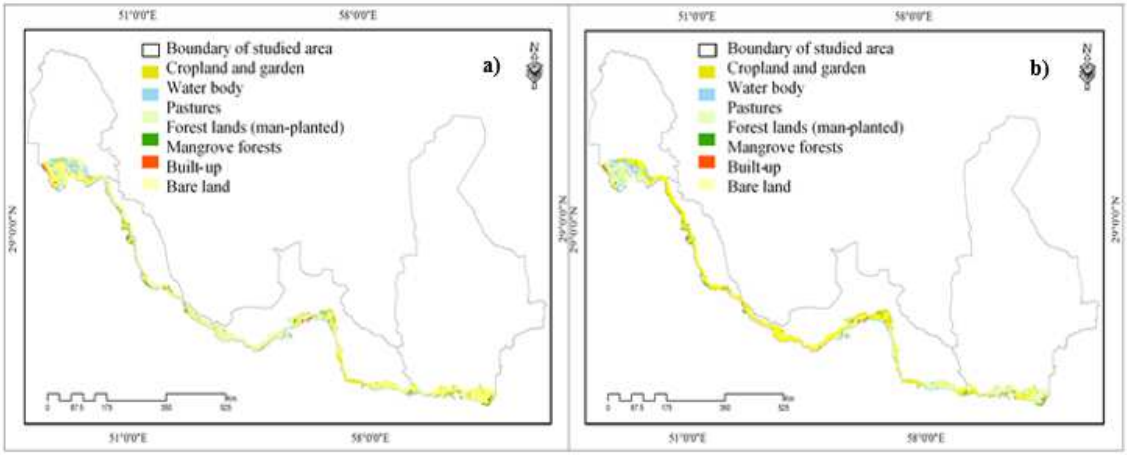


Fig. 3. Forecast map of LULC classes of Iran's mangrove forests during the years: a) 2024 and b) 2050

4.3. Investigating function and equivalence between LULC classes in the area

This section evaluates the function and equivalence (ecological balance) between LULC classes in the area during the studied years (Table 7). According to the results obtained, the equivalence factors were relatively constant, while the function factors fluctuated significantly. Accordingly, among the existing LULCs, pastures had the highest equivalence coefficient and showed the greatest reduction in area during this period. Mangrove forests had the highest functional coefficient among LULCs because of their size.

4.4. Assessment of EF, BC and ED

According to the results, the highest consumption of resources is related to cropland products and pastures. Subsequently, built-up areas show the highest EF among LULC classes (Table 8). Overall, the EF in Iranian mangrove forests (from 1989 to 2024) has an increasing trend, and BC and ED also have a decreasing trend (Fig. 4).

Table 7. Function factor and equivalence among LULC classes in the area

Classes/ Year	Yield Factors (YF)			Equivalence Factors (EQF)		
	1989	2024	2050	1989	2024	2050
Croplands and gardens	0.36	2.25	2.37	1.43	3.22	3.36
Water areas	0.45	2.86	3.02	3.52	3.46	3.18
Pastures	0.32	3.05	3.18	4.23	4.11	2.26
Forests (man-planted)	0.89	3.56	4.05	4.32	4.08	2.85
Mangrove forests	0.23	2.53	2.58	2.74	2.63	2.32
Built-up areas	0.85	3.67	4.15	2.54	4.23	4.36
Bare lands	0.82	3.62	4.08	2.50	4.18	4.23

Table 8. The results of EF, BC and ED in the area (1989-2050)

Year	Classes	1989			2024			2050		
Resource		EF	BC	ED	EF	BC	ED	EF	BC	ED
Biological	Croplands	10156	23456	+13300	12532	25119	+12587	14781	25324	+10534
	Pastures	11421	24874	+13453	12756	25317	+12561	14856	26114	+11258
	Forests	13068	26887	+13819	14357	27436	+13079	15632	27856	+12224
Water	Water for drinking, agriculture and industry	1065	987	-78	1018	863	-155	936	734	-202
Energy	Carbon sequestration	11124	0	0	13568	0	0	14345	0	0
Pollutants	Greenhouse gas emissions	10536	0	0	13167	0	0	14568	0	0
Built-up areas	Anthropogenic areas	11048	0	0	12884	0	0	13254	0	0
Total		**74418**	**78859**	**37149**	**80282**	**76080**	**38072**	**88372**	**72028**	**33823**

EF: Ecological Footprint, BC: Biocapacity, ED: Ecological Deficit, +: Ecological Surplus, -: Ecological Deficit

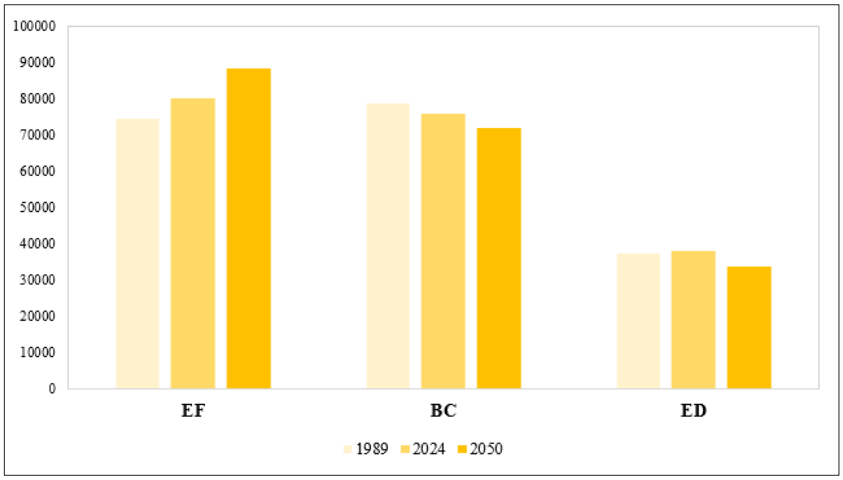


Fig. 4. Trends of EF, BC and ED in the area (1989-2050)

4.5. Assessment of EDI

As the results indicate, the EF increased from 1989 to 2050, which shows a high intensity of resource use (Table 9). The EDI also shows an increasing trend, which indicates an increase in the intensity of natural capital consumption and a decrease in capital accumulation during the studied years. Additionally, during these years, pastures were allocated to the largest share of natural capital, which could be due to the large extent of this land use in the area. However, over time, the natural capital flows of mangrove forests have shown a decreasing trend owing to the development of human activities and conversion of LULC classes, while built-up areas have an increasing trend.

4.6. Assessment of EPI and ESI

According to the results obtained, the EPI has increased in the mangrove forests of Iran during 1989–2050, while the ESI shows a decreasing trend (Table 10). Therefore, the results obtained indicate an increase in EP and a decrease in ES in the area. Among LULC classes, mangrove forests demonstrate the highest sustainability, while pastures show increasing unsustainability over time and also have a decreasing trend.

Table 9. The results of EF and EDI in the area (1989-2050)

Year	1989		2024		2050	
Classes	**EF**	**ED**	**EF**	**ED**	**EF**	**ED**
Croplands and gardens	825	4.73	840	5.18	874	5.36
Water areas	675	1.2	834	1.58	887	1.76
Pastures	789	3.32	926	4.32	954	3.95
Forests (man-planted)	884	4.80	968	5.37	986	4.88
Mangrove forests	487	3.37	568	3.87	823	4.11
Built-up areas	1032	5.41	1147	5.86	1206	5.94
Bare lands	912	4.23	1011	4.98	1128	5.32

EF: ecological footprint, ED: ecological deficit.

Table 10. ESI status based on LULC classes in the area (1989-2050)

Year	1989			2024			2050		
Classes	**EB**	**EP**	**ES**	**EB**	**EP**	**ES**	**EB**	**EP**	**ES**
Croplands and gardens	0.67	0.58	0.75	0.52	0.72	0.57	0.46	0.87	0.48
Water areas	0.54	0.63	0.52	0.43	0.70	0.42	0.37	0.78	0.33
Pastures	0.38	0.90	0.42	0.28	0.98	0.33	0.23	1.05	0.27
Forests (man-planted)	1.23	0.36	0.94	1.11	0.45	0.87	1.02	0.58	0.73
Mangrove forests	1.38	0.30	0.98	1.24	0.42	0.90	1.08	0.53	0.85
Built-up areas	0.72	0.43	0.65	0.64	0.81	0.64	0.54	0.88	0.58
Bare lands	0.58	0.65	0.58	0.48	0.86	0.52	0.37	0.92	0.47

EB: ecological balance, EP: ecological pressure, ES: ecological sustainability.

Subsequently, the capital accumulation to flow indices, flow occupancy ratio, and excess natural capital flow were examined in the studied area (Table 11). According to the results, the use of capital accumulation to flow increased from 1989 to 2050. On the other hand, among the existing LULC, built-up areas and bare lands represent an excess EF and an increase in the cost of BC in the area.

5. Discussion

The resources available to humans for exploitation are very limited, and these limited resources are being destroyed and polluted day by day due to excessive and incorrect use. In other words, natural ecosystems have a limited capacity for humans to use these valuable biological reserves (Elisha & Felix, 2020). Given that Iran's mangrove forests are always exposed to threats from the development of human activities, it is essential to examine the trend of LULC changes and predict the continuation of these changes in the coming years. Accordingly, in the present study, the trend of LULC changes from 1989 to 2024 was examined, as well as the prediction and modeling of these changes in 2050. Next, the EF, BC, ED, and level of EF and balance in this area were calculated. Finally, EPI and ESI were also examined.

According to the results, the area of Iran's mangrove forests in 2024 (with an area of 131.25 km^2 and 0.43%) has decreased compared to 1989 (with an area of 135.54 km^2 and 0.44%). Among the existing LULC classes, built-up areas (with an area of 14032.32 km^2 and 46.40%) have the highest increasing trend, while pastures (with an area of 11438.62 km^2 and 37.82%) have the highest decreasing trend during the years 1989 to 2024. Similarly, in the studies by Mengist et al. (2023) and Jamal Faruque et al. (2022), changes in LULC were identified as the main factors in the decline of mangrove forests. These results show that the development of human activities has led to adverse effects on forest ecosystems and has also increased the trend of LULC changes in the area.

Table 11. Capital stock-to-flow indicators, flow occupancy ratio, and natural capital flow excess in the area (1989-2050)

Year	1989			2024			2050		
Classes	**CSf**	**FOr**	**NCfs**	**CSf**	**FOr**	**NCfs**	**CSf**	**FOr**	**NCfs**
Croplands and gardens	3.84	100	0	4.11	100	0	4.85	100	0
Water areas	3.54	0.91	0	4.05	0.96	0	4.23	1.04	0
Pastures	3.26	0.87	0	3.87	0.92	0	4.11	0.98	0
Forests (man-planted)	4.23	0.98	0	4.45	100	0	4.56	100	0
Mangrove forests	4.48	100	0	4.87	100	0	4.94	100	0
Built-up areas	3.11	0.88	0.70	3.36	0.96	0.87	3.45	1.05	0.92
Bare lands	2.87	0.84	0.63	3.26	0.90	0.75	3.34	0.98	0.84

CSf: Capital stock-to-flow, FOr: Flow occupancy ratio, NCfs: Natural capital flow surplus.

As the results show, in the Iranian mangrove forests, the most decreasing trend in 2050 is related to pastures with an area of 11415.26 km^2 (37.74%), while the largest increasing trend is related to built-up areas with an area of 14056.47 km^2 (46.48%). This trend indicates the speed of development of human activities in these habitats and the conversion of LULC classes to built-up areas. In this regard, Yaghoubzadeh et al. (2022) also referred to these results, stating that mangrove forests are affected by commercial and tourist wharves as the main factor of land change and conversion in the region, and thus these habitats are decreasing and disappearing due to the development of human activities and man-made lands. In addition, Erfanifard and Lotfi Nasirabad (2022) evaluated the spatial and temporal changes of mangrove forests, and the results obtained indicate an increasing trend in changes in these forests under the influence of the development of ecological barriers, especially human activities. It should be noted that the prediction of LULC changes until 2050 is accompanied by uncertainties. The CA-Markov model is based on the assumption that the trends observed in the base period will continue in the future, while factors such as climate change, management policies, infrastructure development, economic developments, and unexpected events can affect the path of changes. Therefore, the results presented for 2050 should be interpreted as a probable scenario based on past trends and not as a definitive prediction. Performing scenario analysis and sensitivity analysis in future research can increase the reliability of predictions.

According to the results obtained, the equivalence factors were relatively constant, while the function factors fluctuated significantly. Accordingly, among the existing LULCs, pastures had the highest equivalence coefficient and showed the greatest reduction in area during this period. Mangrove forests had the highest functional coefficient among LULCs because of their size. Overall, the EF in Iranian mangrove forests (from 1989 to 2024) showed an increasing trend, and BC and ED also had a decreasing trend. The study by Sobhani & Danehkar (2024) in the mangrove forests of the Khamir and Qeshm basins also indicated that the EF has been increasing in recent decades, while BC resources have been decreasing.

As the results show, the EDI also has an increasing trend, which indicates an increase in the intensity of natural capital consumption and a decrease in capital accumulation during the studied years. Additionally, during these years, pastures were allocated to the largest share among natural capital, which could be due to the large extent of this land use in the area. On the other hand, over time, the natural capital flows of mangrove forests have shown a decreasing trend due to the development of human activities and the conversion of LULC classes, while built-up areas have an

increasing trend. The results of the study by Xia et al. (2020) also showed that the existence of incompatible land uses and infrastructure development is the most important threat to mangrove forest ecosystems and their biological resources. In another study, Tran et al. (2024) stated that the main factors of threat and change in mangrove forests are the increasing demand of human communities and the development of built-up areas in these natural habitats, which have led to the reduction of these valuable reserves. In addition, the results obtained indicate an increase in ecological pressure and a decrease in sustainability in the region. Among land uses, mangrove forests are the most stable, while pastures show an unstable state over time and are also on a decreasing trend.

6. Conclusion

According to the results, increasing demand and human-made lands have led to significant changes in the development and transformation of LULC classes in Iran's mangrove forests. In addition, the continuation of these changes until 2050 will lead to an increase in the ecological footprint and a decrease in natural capital in the area. Therefore, achieving sustainable development and protection of natural resources, as well as establishing a balance between human resource consumption and the absorption of waste produced by nature, requires the performance of planners and officials in preserving and supporting these natural habitats, in a way that they strive to preserve their valuable biological resources and improve the conservation status of the forests.

Reference

Ao, Y., Li, H., Zhu, L., Ali, S. & Yang, Z., 2019. The Linear Random Forest Algorithm and Its Advantages in Machine Learning Assisted Logging Regression Modeling, Journal of Petroleum Science and Engineering, 174, 776–789. (https://doi.org/ 10.1111/gcb.15571).

Arifanti, V. B., Basyuni, M., Suharti, S., Slamet, B., Karlina, E., Sidik, F. & Ali, H. M., 2025. Assessing the Environmental and Socioeconomic Impacts of Mangrove Loss in Indonesia: A Synthesis for Science-Based Policy. Forest Science and Technology, 1-17. (https://doi.org/10.22092/wmej.2019.128009.1267).

Arkhi, S. & Esfahani, M., 2019. Forecasting land use changes using multi-temporal images and the Marko chain model (Case Study: Ilam city), Journal of Geography and Territorial Spatial Arrangement (GTSA), 9(30), 95-112. (https://doi.org/10.1016/ j.ecoinf.2023.102324).

Aslami, F., Ghorbani, A., Sobhani, B. & Panahandeh, M., 2015. Comparing artificial neural network, support vector machine and object-based methods in preparation land use/cover mapsusing landSat-8 images, Journal of RS & GIS Techniques in Natural Resources, 6(3), 1-14. magiran.com/ p1488940 (https://doi.org/10.1016/j.petrol. 2018.11.067).

Bi, M., Yao, C., Xie, G., Liu, J. & Qin, K., 2021. Improvement and application of the three-dimensional ecological footprint model. Ecological Indicators, 125, 107480.

Chamberland-Fontaine, S., Estrada, G. T., Heckadon-Moreno, S., & Hickey, G. M., 2022. Enhancing the sustainable management of mangrove forests: The case of Punta Galeta, Panama. Trees, Forests and People, 8, 100274. (https://doi.org/10.1016/j.scitotenv.2018.04.277).

Dang, X., Wu, Y., Liu, G., Yang, Q., Yu, X., & Jia, Y., 2018. Spatial-temporal changes of ecological footprint in the Loess Plateau after ecological construction between 1995 and 2010. Geogr. Res, 37(4), 761-771. (https://doi.org/10.1007/s10668-019-00535-w).

Dong, J., Zhang, Z., Zhang, H., Gao, F., Zhang, W., & Gong, W., 2021. Sustainable utilization and driving mechanism of natural capital in ecologically fragile areas: a case study of Ningxia. China Popul. Resour. Environ, 2, 162-173. (https://doi.org/ 10.3390/rs14194912).

Elisha, O. D., & Felix, M. J. 2020. The loss of biodiversity and ecosystems: a threat to the functioning of our planet, economy and human society. International Journal of Economics, Environmental Development and Society, 1(1), 30-44. (https://doi.org/10.1016/j.oceano.2020.10.003).

Erfanifard, Y., & Lotfi Nasirabad, M., 2022. Efficiency of mangrove indices in mapping some mangrove forests using Landsat 8 imagery in southern Iran. Journal of RS and GIS for Natural Resources, 13(4), 13-16. (In Persian). (https://doi.org/10.1016/j.fuel.2023.127712).

Fischer, J., Wirtz, S. & Scherer, V., 2023. Random Forest Classifier and Neural Network for Fraction Identification of Refuse-Derived Fuel Images, Fuel, 341, 127712. (https://doi.org/10.1016/j.ecss.2020.106644).

Gabisa, M., Kabite, G., & Mammo, S., 2025. Land use and land cover change trends, drivers and its impacts on ecosystem services in burayu sub city, Ethiopia. Frontiers in Environmental Science, 13, 1557000. (https://doi.org/10.1016/j.envc.2021.100419).

Galdavi, S., Akbari, M., Memarian, H., Noughani, M. A., & Aghajani, H., 2025. Analysis of environmental sustainability using ecological footprint and bio-carrying capacity. Journal of Rangeland Science, 15(3). (https://doi.org/10.1111/ddi.13631).

Galli, A., Iha, K., Pires, S. M., Mancini, M. S., Alves, A., Zokai, G., & Wackernagel, M., 2020. Assessing the ecological footprint and biocapacity of Portuguese cities: Critical results for environmental awareness and local management. Cities, 96, 102442. (https://doi.org/10.11594/jtls.07.03.14).

Genta, C., Favaro, S., Sonetti, G., Fracastoro, G. V., & Lombardi, P., 2022. Quantitative assessment of environmental impacts at the urban scale: the ecological footprint of a university campus. Environment, Development and Sustainability, 24(4), 5826-5845. (https://doi.org/10.1016/S0964-5691 (01)00071-0).

Jamal Faruque, Md., Vekerdy, Z., Yeasir Hasan, Md., Islam, K. Z., Young, B., Tofayal Ahmed, M., Monir, M. D., Shovon, Sh. M., Kakon, J. F. & Kundu, P., 2022. Monitoring of land use and land cover changes by using remote sensing and GIS techniques at human-induced mangrove forests areas in Bangladesh. Remote Sensing Applications: Society and Environment, 25, 100699. (https://doi.org/10.1111/geb.12449).

Khezri, M., Mamghaderi, M., Razzaghi, S. & Heshmati, A., 2023. Comprehensive environmental assessment index of ecological footprint. Environmental Management, 71(2), 465-482. (https://doi.org/10.1016/j.sbspro. 06.109).

Lacaux, J. P., Tourre, Y. M., Vignolles, C., Ndione, J.A. & Lafaye, M., 2007. Classification of Ponds from High-Spatial Resolution Remote Sensing: Application to Rift Valley Fever epidemics in Senegal, Remote Sens. Environ, 106, 66–74. (https://doi.org/10.1016/j.ecolind. 2018.01.047).

Lazarus, E., Lin, D., Martindill, J., Hardiman, J., Pitney, L., & Galli, A., 2015. Biodiversity loss and the ecological footprint of trade. Diversity, 7(2), 170-191(https://doi.org/ 20.1001.1.20087845.1402.12.46.10.4)..

Li, X., Li, S., Li, C., Shi, J. & Wang, N., 2023. The impact of high-quality development on ecological footprint: An empirical research based on STIRPAT model. Ecological Indicators, 154, 110881.

Liu, J., Dietz, T., Stephen, R., Carpenter, S.R. & Taylor, W.W., 2007. Complexity of Coupled Human and Natural Systems, Science, 317(5844). (https://doi.org/10.1007/s10311-021-01326-4).

Long, X., Yu, H., Sun, M., Wang, X. C., Klemeš, J. J., Xie, W. & Wang, Y., 2020. Sustainability evaluation based on the Three-dimensional Ecological Footprint and Human Development Index: A case study on the four island regions in China. Journal of Environmental Management, 265, 110509. (https://doi.org/ 10.1016/j.heliyon.2023.e13297).

Lu, D., Mausel, P., Batistella, M., Moran, E., 2004. Comparison of land-cover classification methods in the Brazilian Amazon basin, Photogrammetric Engineering & Remote Sensing, 70(7), 723-731. (https://doi.org/ 10.22108/gep.2022.130601.1458).

Mancini, M. S., Galli, A., Coscieme, L., Niccolucci, V., Lin, D., Pulselli, F. M., & Marchettini, N., 2018. Exploring ecosystem services assessment through Ecological Footprint accounting. Ecosystem Services, 30, 228-235.(https://doi.org/10.1007/978-3-030-85099-9_35).

Mengist, W., Soromessa, T. & Feyisa, G. L., 2023. Forest fragmentation in a forest Biosphere Reserve: Implications for the sustainability of natural habitats and forest management policy in Ethiopia. Resources, Environment and Sustainability, 8, 100058. (https://doi.org/10.1146/annurev.energy.28.0 50302.105459).

Monfreda, C., Wackernagel, M. & Deumling, D., 2004. Establishing national natural capital accounts based on detailed ecological footprint and biological capacity assessments. Land use policy, 21(3), 231-246. (https://doi.org/10.1126/science.1144004).

Muhirwa, F., Li, L., & Laspidou, C., 2025. Global ecosystem sustainability indexing and patterns in the success of SDGs of water, energy and food security. Journal of Cleaner Production, 145830. (https://doi.org/10.1016/ j.ecss.2020. 106644).

Munthali, M., Mustak, Sk., Abiodun, A. & Davis, N., 2020. Modelling Land Use and Land Cover Dynamics of Dedza District of Malawi Using Hybrid Cellular Automata and Markov Model, Remote Sensing Applications Society and Environment, 17(4), 100276. (https://doi.org/ 10.1177/0018720819856454).

Naderi, M. H., Zakerinia, M. & Salarijazi, M., 2019. Aquatic of ecosystem management and restoration rivers. Journal of Ecohydrology,

6(3), 719-737. (In Persian). (https://doi.org/ 10.1016/j.pce.2021.103021).

Nuissl, H., & Siedentop, S., 2021. Urbanisation and land use change. Sustainable land management in a European context: a co-design approach, 75-99. (https://doi.org/10. 1016/j.rse.2017.04.009).

Oli, D., Gyawali, B., Neupane, B. & Oshikoya, S., 2025). Assessment of land use land cover change and its impact on variations of land surface temperature in Atlanta, USA. Environmental and Sustainability Indicators, 100712. (https://doi.org/10.1016/j.indic.2023.100293).

Rondon, M., Ewane, E. B., Abdullah, M. M., Watt, M. S., Blanton, A., Abulibdeh, A. & Mohan, M., 2023. Remote sensing-based assessment of mangrove ecosystems in the Gulf Cooperation Council countries: a systematic review. Frontiers in Marine Science, 10, 1241928. (https://doi.org/ 10.1016/j.scs.2021.103296).

Sagar, S., Roberts, D., Bala, B. & Lymburner, L., 2017. Extracting the Intertidal Extent and Topography of the Australian Coastline from a 28 Year Time Series of Landsat Observations, Remote Sensing of Environment, 195, 153–169. (http://dx.doi.org/ 10.1016/j.apgeog.2005. 11.005).

Sarwar, N., Junaid, A. & Alvi, S., 2024. Impact of urbanization and human development on ecological footprints in OECD and non-OECD countries. Heliyon, 10(19). (https://doi.org/ 10.1016/j.rse.2017.04.009).

Shamaee, S. H., Yousefi, H. & Zahedi, R., 2024. Assessing urban development indicators for environmental sustainability. Discover Sustainability, 5(1), 341. (https://doi.org/ 10.1177/0018720819856454).

Shimu, S.A., Aktar, M., Afjal, M.I., Nitu, A.M., Uddin, M.P. & Al Mamun, M., 2019. NDVI Based Change Detection in Sundarban Mangrove Forest Using Remote Sensing Data, In 2019 4th International Conference on Electrical Information and Communication Technology (EICT), 1-5. IEEE. (https://doi.org/ 10.1016/j.scs.2021.103296).

Sobhani, P. & Esmaeilzadeh, H., 2021. Evaluation and Analysis of Land Use Change Trends in Protected Areas (Case Study: Lar National Park). Iranian Journal of Remote Sensing & GIS, 13(2), 75-92. (In Persian). (https://doi.org/ 10.1016/j.rse.2017.04.009).

Sobhani, P. & Danehkar, A., 2024. Evaluation of Natural Capital Changes and Ecological Sustainability in the Hara Protected Area. Geography and Environmental Sustainability, 14(2), 49-63. (In Persian). (https://doi.org/ 10.1177/0018720819856454).

Sobhani, P. & Danehkar, A. 2025. Foresight and development scenarios based on ecosystem services in Iranian mangrove forests. Geographical spatial planning. Online publication. (In Persian). (https://doi.org/10. 1016/j.scs.2021.103296).

Sobhani, P., Esmaeilzadeh, H., & Mostafavi, H., 2021. Simulation and impact assessment of future land use and land cover changes in two protected areas in Tehran, Iran. Sustainable Cities and Society, 75, 103296. (https://doi.org/10.1016/j.indic.2023.100293).

Tran, T. V., Reef, R. & Zhu, X., 2024. Long-term changes of mangrove distribution and its response to anthropogenic impacts in the Vietnamese Southern Coastal Region. Journal of Environmental Management, 370, 122658. (https://doi.org/10.1016/j.ecolind.2020.106196).

Wang, L., Wei, F., Tagesson, T., Fang, Z. & Svenning, J. C., 2025. Transforming forest management through rewilding: Enhancing biodiversity, resilience, and biosphere

sustainability under global change. One Earth, 8(3). (https://doi.org/10. 28930/jitkt.v3i2.7818).

Wassie, S. B., 2020. Natural resource degradation tendencies in Ethiopia: a review. Environmental systems research, 9(1), 1-29. (http://dx.doi.org/ 10.1016/ j.apgeog.2005.11.005).

Wu, F., Yang, X., Shen, Z., Bian, D. & Babuna, P., 2021. Exploring sustainability and decoupling effects of natural capital utilization in China: Evidence from a provincial three-dimensional ecological footprint. Journal of Cleaner Production, 295, 126486. (https://doi.org/ 10.1080/15481603. 2021.2022427).

Xia, Q., Qin, C.Z., Li, H., Huang, C., Su, F.Z. & Jia, M.M., 2020. Evaluation of Submerged Mangrove Recognition Index Using Multi-Tidal Remote Sensing Data, Ecol. Indic., 113, 106196.

Xie, H., Sun, Q. & Song, W., 2024. Exploring the Ecological Effects of Rural Land Use Changes: A Bibliometric Overview. Land, 13(3), 303. (https://doi.org/10.1016/j.ecolind. 2020.106196).

Yadav, M., 2023. Assessment of Urban Growth and Ecological Sustainability: Insights from Mumbai, India. Assessment, 10 (8), 404-418. (https://doi.org/10.28930/jitkt.v3i2.7818).

Yaghoubzadeh, M., Salmanmahiny, A., Mikaeili Tabrizi, A., Danehkar, A. & Moslehi, M., 2022. Prioritizing environmental hazards of mangrove forests in Hormozgan province. Journal of Natural Environmental Hazards, 10(30), 69-82 (In Persian). (https://doi.org/ 10.1016/j.indic.2023.100293).

Yang, H., Yan, S., An, N. & Yao, Q., 2024. Using ecological footprint analysis to evaluate sustainable development in Lushan county, China. Land, 13(7), 1081. (https://doi.org/ 10.1016/j.ecolind.2020.106196).

Yang, Y. & Hu, D., 2018. Natural capital utilization based on a three-dimensional ecological footprint model: A case study in northern Shaanxi, China. Ecological indicators, 87, 178-188.(https://doi.org/ 10.1016/ j.scs.2021.103296).

Zadehdabagh, N., Monavari, S. M., Kargari, N., Taghavi, L. & Pirasteh, S., 2022. Sustainability of agroecosystems by indices: A comparative study between indicators of ecological footprint sustainability and emergy analysis; a case study in Dez catchment, Iran. Ecological Modelling, 474, 110165. (https://doi.org/10.1080/ 15481603. 2021.2022427).

Zhang, L., Huettmann, F., Liu, S., Sun, P., Yu, Z., Zhang, X. & Mi, C., 2019. Classification and Regression with Random Forests as a Standard Method for Presence-Only Data SDMs: A Future Conservation Example Using China Tree Species, Ecological Informatics, 52, 46–56. (https://doi.org/ 10.1177/00187208 19856454).

Zheng, Y., Takeuchi, W. & Jiang, Q., 2023. Assessing mangrove conservation in China by integrating mangrove ecosystem into ecological footprint accounting. Ocean & Coastal Management, 242, 106728. (http://dx.doi.org/10.1016/j.apgeog.2005.11.005).

Zhu, L., Zhang, H., Liao, H. & Peng, R., 2020. Evaluation of ecological sustainability in Chongqing, China based on 3D ecological footprint model. International Journal of Design & Nature and Ecodynamics, 15(1), 89-96. (https://doi.org/10.28930/jitkt.v3i2.7818).